Dispersive Character of Optical Phonons in GaAlAs Alloys from Raman Scattering in Superlattices

Bernard Jusserand, Daniel Paquet,[a] and Francis Mollot
Groupement Scientifique du Centre National d'Etudes des Télécommunications et du Centre National de la Recherche Scientifique, Laboratorie de Bagneux, 196 Avenue Henri Ravera, 92220 Bagneux, France
(Received 17 July 1989)

We demonstrate for the first time the well-defined dispersive character of optical phonons in III-V mixed crystals. Raman scattering on short-period GaAlAs/AlAs superlattices evidences several modes confined in the alloy layers. This determines experimental points on the bulk-alloy phonon dispersion curves in agreement with the predictions of a coherent-potential-approximation calculation which takes into account both disorder and superlattice effects.

PACS numbers: 63.20.Dj, 63.50.+x, 78.30.Fs, 78.65.Fa

We prove experimentally and theoretically for the first time that in III-V mixed crystals exhibiting an optical-phonon two-mode behavior,[1] these modes, although originating from disorder effects, exhibit a well-defined dispersion. The zone-center properties of these vibrations have been extensively studied by Raman scattering on bulk alloys, particularly on $Ga_{1-x}Al_xAs$. The most recent investigations[2,3] have considered the asymmetric profile of the bulk-alloy Raman lines. Parayantal and Pollak[2] obtained an excellent description of these profiles using a spatial-correlation model. In this analysis, the broad zone-center spectra of the alloys result from the disorder-induced relaxation of the $q=0$ wave-vector selection rule which applies in pure compounds. This strict selection rule was replaced in Ref. 2 by a Gaussian distribution and the asymmetric profile of the GaAs-type lines thus originates in the downwards dispersion of the LO phonons in pure GaAs. On the other hand, we previously obtained[3] a good description of this asymmetry using a different approach, namely, an alloy lattice-dynamics calculation based on the coherent-potential approximation (CPA), which we will describe further below. Using either description (spatial-correlation or CPA model), one should predict the persistence of some downwards dispersion of the optical modes in the GaAlAs alloy. Up to now, however, there has been no experimental information on the well-defined character nor on the shape of the dispersion of these alloys optical vibrations.

As the usual method of neutron scattering appears very difficult to apply on such alloys, which unfortunately are not available as homogeneous large samples, we chose to insert the investigated $Ga_{1-x}Al_xAs$ alloys into a periodic $GaAs/Ga_{1-x}Al_xAs$ superlattice. Indeed it is well known[4] that for pure compound superlattices like $(GaAs)_{n1}/(AlAs)_{n2}$, Raman backscattering spectra display several peaks associated to longitudinal-optical vibrations (LO) confined in the individual layers. Their frequencies correspond to the bulk LO ones at different finite wave vectors:[5]

$$k_p^{1,2}=p\pi/(n_{1,2}+1)a\,, \tag{1}$$

where a is the monolayer thickness and $n_{1,2}a$ are the respective thicknesses of the GaAs and AlAs layers in the supercell. This allows one to obtain from a single Raman scattering experiment several points on the dispersion curves of the bulk constituents. This analysis is only valid when the allowed optical bands of the two constituents are well separated in frequency, and when interfaces are abrupt.[6]

On the other hand, our lattice-dynamics calculation,[3] based on a shell model[7] and a CPA treatment of disorder,[8] predicts the following: (1) For any given composition x, the alloy exhibits an optical-phonon two-mode behavior with two zone-center LO frequencies $\omega_{Ga}(x)$ and $\omega_{Al}(x)$ which lie, respectively, somewhat below the pure GaAs and AlAs zone-center ones. (One gets similar results for TO modes, which, however, will not be considered in this Letter.) (2) One can define[9,10] from the CPA spectral density of state (SDOS) thick, but well-defined dispersion curves for both modes, which both display a downwards variation as the wave vector increases from the zone center. In Fig. 1 we plot the calculated dispersion curves along the superlattice axis of the GaAs-type LO phonon in GaAs, $Ga_{0.85}Al_{0.15}As$, and $Ga_{0.7}Al_{0.3}As$, deduced from the energy of the maximum SDOS at each wave vector. For $x=0.15$, we also indicate the thickness of the dispersion curve through a hatched surface limited by the half-maximum SDOS energies. This thickness at zone center reproduces well the asymmetric line shape observed on bulk alloys.[3] (3) The bandwidth of each mode roughly scales with the concentration of the corresponding cation, as is also apparent in Fig. 1. As a consequence, the GaAs-type band in the alloy is well separated in frequency from the pure AlAs one and one can expect, and we shall actually prove it, that the preceding analysis [Eq. (1)] can also be applied to the alloy case. On the contrary, the AlAs-type band

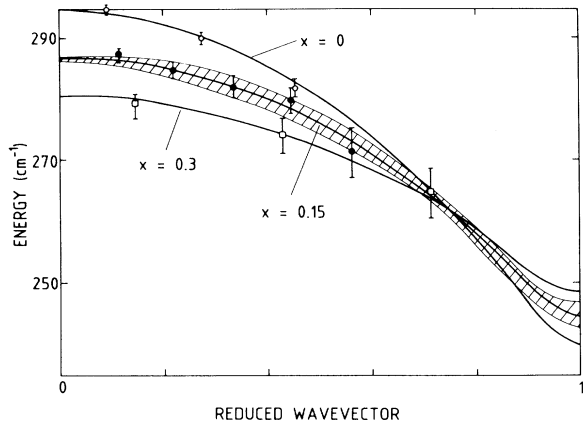

FIG. 1. Calculated dispersion curves along the superlattice axis of the GaAs-type LO phonon in bulk $Ga_{1-x}Al_xAs$ mixed crystals, with $x=0$, 0.15, and 0.30. For $x=0.15$, the hatched surface reflects the thickness of the dispersion curve, as explained in the text. Open circles, solid circles, and open squares correspond to experimental frequencies, respectively, of samples A, B, and C, plotted according to Eq. (1).

overlaps the pure AlAs one and the corresponding superlattice modes are propagative and will not be considered in what follows.

We performed Raman scattering experiments on three samples grown by molecular-beam epitaxy: a reference sample $(GaAs)_{10}/(AlAs)_4$ (sample A) and two others containing alloys, $(Ga_{0.85}Al_{0.15}As)_8/(AlAs)_4$ (sample B) and $(Ga_{0.70}Al_{0.30}As)_6/(AlAs)_4$ (sample C). We chose to decrease the alloy thickness when the Ga content decreased to roughly compensate the decrease of the GaAs-type bandwidth by an increase in the wave-vector sampling periodicity $\pi/(n_{1,2}+1)a$ according to Eq. (1). We show in Fig. 2, spectrum a, the Raman spectrum in the GaAs LO frequency range obtained on sample A in the $z(x,y)\bar{z}$ configuration, using the 514-nm line of an Ar^+-ion laser. We indexed the lines with the associated values of p [Eq. (1)], which are odd as they correspond to the allowed B_2 modes in this configuration.[4] The even-index modes are allowed in the $z(x,x)\bar{z}$ configuration but remain rather weak except for some specific resonant conditions.[11] We also plot in Fig. 1 the experimental results $\omega(k_p)$ compared with the bulk GaAs dispersion curves deduced from our shell model, after adjusting the experimental zone-center frequency, and we conversely plot the predicted frequencies $\omega(k_p)$ on the experimental spectrum a in Fig. 2.

We observed some similar structures on samples B and C in the perpendicular configuration, as illustrated by Fig. 2, spectra $b\perp$ and c (spectra recorded at 476-nm incident wavelength). Furthermore, we observed on sample B some weaker signal for the 514-nm line in the $z(x,x)\bar{z}$ configuration (see Fig. 2, spectrum $b\parallel$). The spectrum actually displays two maxima at frequencies between those of lines 1, 3, and 5, which we label 2 and

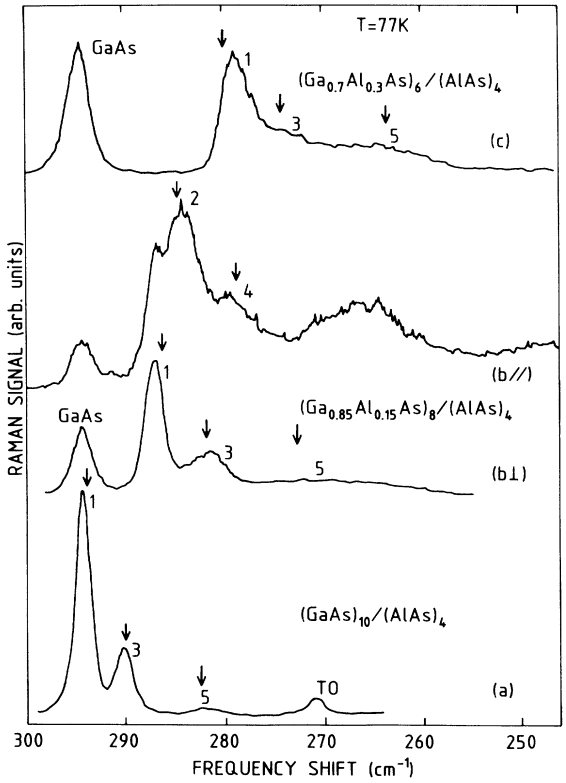

FIG. 2. Raman spectra in the GaAs-type frequency range obtained at liquid-nitrogen temperature in the $z(x,y)\bar{z}$ configuration on sample A (spectrum a), sample B (spectrum $b\perp$), and sample C (spectrum c), and also in the $z(x,x)\bar{z}$ configuration on sample B (spectrum $b\parallel$). The line labelings are used in the text, while the arrows above each labeled line point to the corresponding calculated frequencies. Note that the higher-frequency line labeled GaAs originates from the buffer layer.

4. We assign these structures to A_1 confined modes (even p index) which become observable due to some unidentified resonance, and lines 1, 3, and 5 to the same confined B_2 modes as in sample A. However, this assignment is somewhat uncertain for line 5, which lies at frequencies close to the GaAs TO frequency (see Fig. 2, spectrum a). Indeed the GaAs TO branch, being rather flat, is hardly sensitive to confinement and alloying. In a similar way as for sample A, we plot in Fig. 1 the experimental frequencies $\omega(k_p)$ with respect to the CPA dispersion curves and conversely in Fig. 2 the predicted confined-alloy frequencies in comparison with the spectra. We think that, when considering the experimental uncertainties on the thickness of the layers and the abruptness of the interfaces, the agreement is quite good except perhaps for line 5 in sample B.

Let us now account theoretically for these experimental results. The simplest description one can think of is to describe the superlattice by the periodic stacking of two layers, one which is the pure AlAs compound and

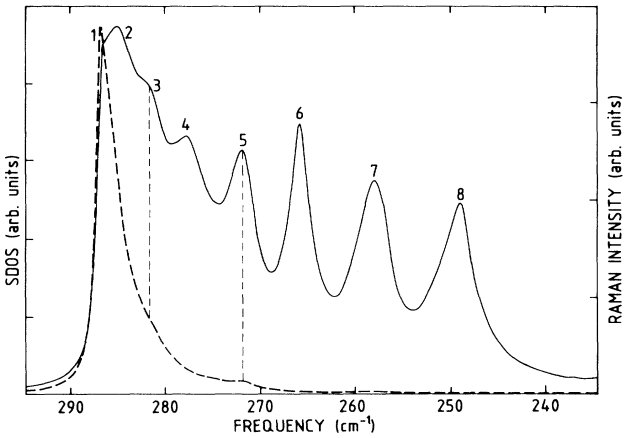

FIG. 3. Spectral density of states (SDOS) of the GaAs-type LO vibrations (full line) and the associated Raman intensity (dashed line), calculated at a vanishingly small wave vector along the superlattice axis. We used the parameters of sample *B* and the bulk CPA mass in the confined alloy layer.

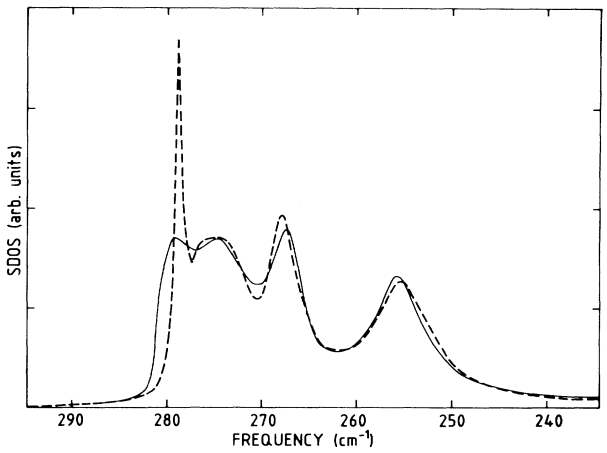

FIG. 4. Spectral density of states (SDOS) of the GaAs-type LO vibrations calculated at vanishingly small wave vector along the superlattice axis with the parameters of the model sample $(Ga_{0.7}Al_{03}As)_4/(AlAs)_2$. We used either the bulk CPA mass (full line) or the superlattice CPA ones (dashed line).

the other which is made of the bulk self-consistent CPA alloy. The latter consists of a fictive ordered crystal which depends only on a frequency-dependent isotropic complex mass assigned to the randomly occupied cation sites. This mass is self-consistently determined when one assumes the force-constant matrix to be independent of the site occupation and if one demands that a given random occupied site imbedded in the CPA effective medium produces no extra scattering on the average. Then, using the Kanellis method,[12] one can easily build up the superlattice dynamical matrix, whose associated Green's function leads to any spectral quantity one is looking for. We plot in Fig. 3, for sample *B*, the longitudinal spectral density of states in the GaAs-mode frequency range for a very small wave vector parallel to the superlattice *z* axis. As expected, this quantity exhibits eight maxima, associated to the eight confined modes, at frequencies in agreement with the predictions of Eq. (1). This fully justifies our previous comparison between the experimental spectra and the bulk CPA dispersion curve. Furthermore, we have computed an estimate of the frequency-dependent Raman intensity, using the bond-polarizability model[4,13] applied to the longitudinal eigendisplacements with a very small wave vector along the growth direction. We assumed no spatial variation for the model coefficients. The result is also plotted in Fig. 3. One gets three structures, associated to lines 1, 3, and 5, which qualitatively reproduce the relative experimental intensities, but which are far less resolved than the experiment.

One can, however, wonder whether the superlattice confinement would affect the alloy average lattice dynamics. Indeed the CPA self-mass is deduced self-consistently from the lattice dynamics it produces and, already in a pure GaAs/AlAs sample, the GaAs-type modes are strongly affected by the confinement. Strictly speaking, a computation of the alloy superlattice lattice dynamics should account for the tetragonal average symmetry and for the nonequivalent randomly occupied cation sites in the supercell. In the case of sample *B* (eight alloy monolayers), taking into account all the symmetries of the structure, one should determine self-consistently four "longitudinal" and four "transverse" CPA masses, associated, respectively, to displacements along the growth axis and in the layer plane. This is a formidable task and very difficult to achieve. To get a qualitative feeling of the influence of the confinement on the disorder-induced Raman linewidth, while remaining within the abilities of a vectorial computer, we chose to study a model superlattice: $(Ga_{0.7}Al_{0.3}As)_4/(AlAs)_2$. One thus has to determine only four independent CPA masses, while retaining the main physics.

The results are illustrated in Fig. 4 where we plot the exact longitudinal SDOS for vanishing wave vector along the superlattice axis in comparison with the one obtained assuming the alloy layer to be bulklike. These longitudinal SDOS's are essentially similar except at high frequencies around the $p=1$ mode, where the "exact" calculation leads to a much better defined line. This line narrowing originates from the fact that the total density of states around $\omega(k_1)$ is very small due both to confinement and to the electrostatic-induced anisotropy.[14] Consequently, the alloy fluctuations can hardly scatter elastically a CPA mode at this energy due to the lack of final states. This is mathematically confirmed by the smallness of the imaginary parts of both the longitudinal and transverse CPA masses which actually become large only for frequencies less than $\omega(k_2)$. We think that this explanation of the narrowing of the $p=1$ line is general and can thus be applied to more complex structures like those we experimentally studied. This full CPA calcula-

tion thus further validates the use of Eq. (1) for predicting the frequency of the modes confined in the alloy layer and moreover explains why the experimental $p=1$ line is quite narrower than predicted by the naive model.

In conclusion, we demonstrated both experimentally and theoretically that GaAs-type optical modes in the $Ga_{1-x}Al_xAs$ mixed crystal exhibit a well-defined downwards dispersion, in agreement with the predictions of the CPA. When the alloy is inserted in a superlattice, the frequencies of the confined modes can be safely account for using a clamped-vibrating-string analogy [Eq. (1)]. However, the confinement and the tetragonal anisotropy of electrostatic origin make the first confined mode less sensitive to disorder and thus better defined than one would naively expect.

---

[a]Deceased.

[1]A. S. Barker and A. J. Sievers, Rev. Mod. Phys. **47**, Suppl. No. 2, S1 (1975), and references therein.

[2]P. Parayantal and F. H. Pollak, Phys. Rev. Lett. **52**, 1822 (1984).

[3]B. Jusserand, D. Paquet, and K. Kunc, in *Proceedings of the Seventeenth International Conference on the Physics of Semiconductors, San Francisco, August 1984,* edited by J. D. Chadi and W. A. Harrison (Springer-Verlag, New York, 1985), p. 1165.

[4]For a review on vibrations in superlattices, see B. Jusserand and M. Cardona, in *Light Scattering in Solids,* edited by M. Cardona and G. Güntherodt (Springer-Verlag, Heidelberg, 1989), p. 49.

[5]B. Jusserand and D. Paquet, Phys. Rev. Lett. **56**, 1751 (1986).

[6]B. Jusserand, F. Alexandre, D. Paquet, and G. Le Roux, Appl. Phys. Lett. **47**, 301 (1986); G. Fasol, M. Tanaka, H. Sakaki, and Y. Horikoshi, Phys. Rev. B **38**, 605 (1988).

[7]K. Kunc and H. Bilz, Solid State Commun. **19**, 1027 (1976).

[8]D. W. Taylor, Phys. Rev. **156**, 1017 (1967).

[9]P. Soven, Phys. Rev. **178**, 1136 (1969).

[10]B. Jusserand, D. Paquet, A. Regreny, and J. Kervarec, Solid State Commun. **48**, 499 (1983).

[11]A. K. Sood, J. Menendez, M. Cardona, and K. Ploog, Phys. Rev. Lett. **54**, 2111 (1985).

[12]G. Kanellis, Phys. Rev. B **35**, 746 (1987).

[13]A. S. Barker, Jr., J. L. Merz, and A. C. Gossard, Phys. Rev. B **17**, 3181 (1978).

[14]R. Merlin, C. Colvard, M. V. Klein, H. Morkoc, A. Y. Cho, and A. C. Gossard, Appl. Phys. Lett. **36**, 43 (1980); S. F. Ren, H. Chu, and Y. C. Chang, Phys. Rev. B **37**, 8899 (1988).